Published in final edited form as:
New Phytol. 2011 January ; 189(2): 616–628. doi:10.1111/j.1469-8137.2010.03511.x.

Possible contributions of *TERMINAL FLOWER 1* to the evolution of rosette flowering in *Leavenworthia* (Brassicaceae)

Ning Liu, **Marek K. Sliwinski**, **Raul Correa**, and **David A. Baum**
Department of Botany, University of Wisconsin, 430 Lincoln Drive, Madison, WI 53706, USA

Summary

- *Leavenworthia crassa* is a rosette flowering species that differs from inflorescence flowering species, such as *Arabidopsis thaliana*, in having elongated pedicels and shortened interfloral internodes on the main axis. Based on previous experiments, we hypothesized that changes to the *L. crassa TFL1* ortholog, *LcrTFL1*, were important in the evolution of rosette flowering.
- We isolated *LcrTFL1* and introduced a genomic construct into *tfl1* mutant *A. thaliana* plants. We also generated and analyzed *EGFP-LcrTFL1* reporter-fusion lines, and *LcrTFL1*/*LcrLFY* doubly transgenic lines.
- The transgene rescued the mutant defects, but manifested gain-of-function phenotypes. However, *LcrTFL1* lines differed from *35S:TFL1* lines in several regards. Defects in floral meristem identity establishment were observed, as was the production of flowers with extra petals. We also noted features that resemble rosette flowering: *LcrTFL1* lines produced significantly shorter interfloral internodes and significantly longer pedicels than either wild-type or *35S:TFL1* plants.
- Our data show that there are substantive differences in the regulation and/or function of *TFL1* orthologs between *A. thaliana* and *L. crassa*. These may reflect changes that occurred during the evolution of rosette flowering in *Leavenworthia*, but, if so, our results show that additional, as-yet-unidentified genes were involved in this instance of architectural evolution.

Keywords

inflorescence evolution; *LEAFY*; meristem identity genes; molecular coevolution; plant architecture; *TERMINAL FLOWER 1*

Introduction

Plants exhibit a range of inflorescence architectures, which play an important role in adaptation to varied environments (Tucker & Grimes, 1999). Theoretical models of plant architecture have suggested that much of the current diversity of inflorescence form can be explained by modulation of very few developmental parameters (Prusinkiewicz *et al.*, 2007). Specifically, if the identity of shoot meristems is controlled by two antagonistic gene products, developmental regulation of the levels of these gene products in parent (i.e. terminal) and daughter (i.e. axillary) meristems can explain almost all the inflorescence

Author for correspondence: David A. Baum, Tel: +1 608 265 5385, dbaum@wisc.edu.

forms seen in angiosperms. The challenge is to connect these theoretical models with empirical data on the developmental genetic basis of inflorescence evolution.

Previous developmental work in model species has suggested that the two most important genes involved in the regulation of meristem identity are homologs of *FLORICAULA*/*LEAFY* (*LFY*), which promotes floral identity, and *CENTRORADIALIS*/*TERMINAL FLOWER 1* (*TFL1*), which promotes vegetative identity (Bradley *et al.*, 1996, 1997; Conti & Bradley, 2007). Genetic data show that early *LFY* expression during bolting activates *TFL1* expression, whereas later in development the two genes act antagonistically such that floral meristems express *LFY* but not *TFL1*, and inflorescence meristems express *TFL1* but not *LFY* (Ratcliffe *et al.*, 1999; Benlloch *et al.*, 2007). The most plausible mechanism by which *TFL1* represses *LFY* is via competition with a close relative of *TFL1*, *FLOWERING LOCUS T* (*FT*). *FT* is part of a transcriptional complex that activates *APETALA1* (*AP1*), which is an important activator of *LFY* expression (Ahn *et al.*, 2006). Conversely, repression of *TFL1* in floral meristems also appears to be mediated by *AP1*: the AP1 protein is thought to bind the 3′ noncoding region of the *TFL1* locus and to directly repress its expression (Kaufmann *et al.*, 2010). These data and models predict that inflorescence evolution will commonly involve changes at the *LFY* or *TFL1* loci and/or genes such as *AP1* that modulate their expression and/or genetic interactions (Coen & Nugent, 1994; Bradley *et al.*, 1996, 1997).

Arabidopsis thaliana and most Brassicaceae produce all their flowers on elongated shoot systems, called inflorescences. Each flower has a short pedicel, and elevation of the flowers above the ground is primarily the result of the elongation of shoot internodes. We will call this architecture ‘inflorescence flowering’ (Fig. 1a). An alternative plant architecture, ‘rosette flowering’, also occurs within Brassicaceae. In rosette flowering species, flowers are borne singly on elongated pedicels that emerge from the rosette. This architecture is illustrated by *Leavenworthia crassa*, which initially produces a rosette containing solitary flowers borne on elongated pedicels (Fig. 1b). These flowers are produced in the axils of cryptic bracts (Bosch *et al.*, 2008) on the flanks of an indeterminate shoot axis (lacking a terminal flower). However, *L. crassa* is best viewed as a partially rosette-flowering species because, if plants are grown in good conditions, they will later produce elongated inflorescences from the axils of basal rosette leaves. Nonetheless, because early development conforms to the rosette flowering architecture, and because *Leavenworthia* represents a clade that transitioned from being ancestrally inflorescence flowering to (partially) rosette flowering, *L. crassa* provides a valid model for studying the evolution of rosette flowering. It has been argued that rosette flowering in Brassicaceae is an adaptation to growing in low-competition environments with short and unpredictable growing seasons (Bosch *et al.*, 2008).

Previous work on the genetic changes underlying the evolution of rosette flowering has focused on independent transitions from inflorescence to rosette flowering in the genera *Ionopsidium*, *Idahoa* and *Leavenworthia.* Based on comparative expression (Shu *et al.*, 2000; Sliwinski *et al.*, 2007; Bosch *et al.*, 2008), molecular evolutionary analysis (Baum *et al.*, 2005), and interspecies transformation experiments (Yoon & Baum, 2004; Sliwinski *et al.*, 2006, 2007), the regulation and/or activity of *LFY* homologs has been shown to have changed in each of the three lineages. However, in no case could the evolution of rosette flowering be attributed only to changes to *LFY* homologs, showing that other genetic players are involved.

Experiments with the *L. crassa LFY* ortholog (*LcrLFY*) suggested a possible role for this gene in internode compression (Sliwinski *et al.*, 2006; Bosch *et al.*, 2008). *A. thaliana lfy* mutants rescued with a *LcrLFY* genomic construct produced terminal flowers. This phenotype was attributed to the 5′ *cis*-regulatory region (‘promoter’) of the *LcrLFY* locus,

which drives expression in the inflorescence meristem, apparently escaping TFL1-mediated repression (Yoon & Baum, 2004). At the same time, the coding region of *LcrLFY* (whether driven by the *LcrLFY* or *LFY* promoter) caused elevated early expression of *TFL1*, suggesting that the LcrLFY protein is more effective than LFY at activating *TFL1* during early development (Sliwinski *et al.*, 2006). Taken together, these data suggested the hypothesis that reciprocal up-regulation of *LFY* and *TFL1* homologs in the *Leavenworthia* lineage contributed to the evolution of rosette flowering (Sliwinski *et al.*, 2006).

In the work reported here, we tested this hypothesis by isolating the *L. crassa TFL1* ortholog (*LcrTFL1*) and analyzing its function in an *A. thaliana* background. Our data are consistent with the prevailing models of *LFY-TFL1* antagonism, and suggest that changes at the *TFL1* locus played a role in internode compression and pedicel elongation. However, *TFL1* and *LFY* are still not sufficient to explain all aspects of rosette flowering in *L. crassa*.

Materials and Methods

Plant materials

Unless otherwise stated, *A. thaliana* seeds were originally obtained from the Arabidopsis Biological Recourse Center (The Ohio State University, Columbus, OH, USA). Transgenic *LcrLFY A. thaliana* were the lines described in Yoon & Baum (2004) and Sliwinski *et al.* (2006). *35S:TFL1* transgenic *A. thaliana* were kindly provided by Prof. Enrico Coen (John Innes Centre, Norwich, UK) and *EGFP-TFL1* was kindly provided by Prof. Koji Goto (Research Institute for Biological Sciences, Okayama, Japan). The latter construct contains green flourescent protein (GFP) inserted at the start of exon 1 of a *TFL1* genomic sequence, complete with non-coding sequences 1920 bp 5′ of the start codon and 5300 bp 3′ of the stop codon (K. Goto *et al.*, pers. comm.). All *Arabidopsis* lines were grown as described previously (Sliwinski *et al.*, 2006).

Leavenworthia crassa Rollins seeds were germinated and grown on prewetted and sterilized filter paper, then kept in a growth chamber at 15:9°C day:night under 16 h photoperiods until germination. Seedlings with two true leaves were transferred to soil and cultivated at 23°C under 16 h photoperiods.

Isolation of *LcrTFL1* and sequence analysis

By using degenerate primers (*TFL1*-DGF, GNAGWGTK RTHGGAGA; *TFL1*-DGR, AAHDYDYKWGTGYTG AA), based on highly conserved regions of *TFL1* genes, we isolated *TFL1* homologs from *L. crassa* genomic DNA. Amplified products were cloned and sequenced to confirm their identity. We then conducted several rounds of genome walking (Clontech, Mountain View, CA, USA) in order to obtain several kilobases of flanking, non-coding sequence both 5′ and 3′ of the coding region. We identified potential *cis*-regulatory elements in the 5′- and 3′-intergenic regions of *LFY* and *LcrLFY* using the plant *cis*-acting element database, PLACE (http://www.dna.affrc.go.jp/PLACE/). We determined the dN:dS ratio using SNAP (http://www.hiv.lanl.gov/content/sequence/SNAP/SNAP.html).

To assess orthology, we built an alignment of *TFL1* homologs, focusing on *A. thaliana*, papaya (*Carica papaya* (*Cpa*)), and poplar (*Populus trichocarpa* and *P. balsamifera* (*Ptr* and *Pba*)), which are all rosids. Homologs from *Physcomitrella patens* (PHYPADRAFT numbers 60404, 120777, 127945, and 134340 (*PpaTFL1-like 1–4*)) were used as outgroups. We downloaded coding sequences and built both DNA and protein alignments starting with an initial alignment in Clustal W (Thompson *et al.*, 1994) using default settings, as implemented in MEGA (Kumar *et al.*, 1994, 2008), followed by a manual adjustment in MacClade 4 (Maddison & Maddison, 2002). Nucleotide and protein alignments are provided (Supporting Information, Figs S1, S2). After removing truncated or partial sequences, we

conducted phylogenetic analyses of both the DNA and protein matrices using MrBayes 3.1 (Huelsenbeck & Ronquist, 2001; Ronquist & Huelsenbeck, 2003) with the CIPRES 2.0 portal (Miller *et al.*, 2009). We initiated two MCMC runs of two million generations, each comprising four linked chains (heat = 0.2) with sampling every thousand generations. The nucleotide data were analyzed using the Generalized Time Reversible model with rate heterogeneity modelled with a discrete approximation to a gamma distribution (GTR + γ). The protein data were analyzed using the Whelan and Goldman (WAG) model. The first 250 trees from the posterior sample of each run were discarded as burn-in, and the remaining trees were used to generate a majority rule consensus tree with clade posterior probabilities. Outgroups were pruned from the phylogeny to save space. The sequence names used for convenience are guided by preliminary phylogenetic results and do not reflect functional data: *CpaTFL1-like*, evm.TU.contig_45053.1; *CpaFT-like*, evm.TU.contig_32595.1; *CpaBFT-like*, evm.TU.supercontig_107.26; *CpaE12A11-like*, EST 1565745_5_G15_058 PY06; *PtrTFL1-like*, NC_008475.1; *PbaTFL1-like*, NW_1492762.1; *PtrBFT-like*, NC_008481.1; *PtrFT-like-1*, NC001491506.1; *PtrFT-like-2*, NW_1491690.1; *PtrFT-like- 3*, NC_008476.1; *PtrMFT-like*, NC_008480.1; *TFL1*, NM_120465; *ATC* (*A. thaliana CENTRORADIALIS*-like), NM_128315; *FT* (*FLOWERING-LOCUS T*), NM_105222; *TSF* (*TWIN SISTER OF FT*), NM_118156; *MFT* (*MOTHER OF FT AND TFL1*), NM_101672; *BFT* (*BROTHER OF FT AND TFL1*), NM_125597.

Cloning, transformation and phenotype scoring

Based on the genomic sequence, we designed primers to amplify the *LcrTFL1* coding region and the entire 5′- and partial 3′-intergenic spacers. Four independent clones (two in each orientation) were generated using the binary vector pPZP211, which includes the *NPTII* selectable marker conferring kanamycin resistance. We also generated reporter constructs in which EGFP was translationally fused to LcrTFL1. The *EGFP* coding sequence was introduced between the 5′-untranslated region (UTR) and the start codon of the *LcrTFL1* genomic sequence. The fusion construct was subcloned into the pCAMBIA3300 vector, which includes the *Bar* selectable marker conferring Basta resistance, and was introduced into *tfl1*-2 plants. T1 seedlings were identified by spraying with a 1:1000 dilution of Finale herbicide (AgrEvo Company, Wilmington, DE, USA).

Arabidopsis thaliana tfl1-2 Landsberg *erecta* (L*er*) homozygous mutant plants were transformed with the four genomic clones using the floral dip method (Clough & Bent, 1998). Primary transformant (T1) plants were selected by seed germination on 0.5× Murashige and Skoog (MS) plates supplemented with 50 mg l^{-1} kanamycin. Each of the four constructs yielded *c.* 50 seedlings exhibiting kanamycin resistance. A subset of these sampled from the four constructs were transferred to soil at 23°C under long-day conditions (16:8 h day:night). The segregation ratio of kanamycin-sensitive (Kan^S) to kanamycin-resistant (Kan^R) offspring from T1 plants was used to estimate the number of transgene loci.

We identified five independent T1 lines in a wild-type background, each inferred to have a single transgene locus. T2 plants from each of these lines were grown on soil in a glasshouse, with a single plant in each 3.25 inch pot. At maturity (50–60 d after planting), plants were scored for the number of paraclades emerging from the elongated portion of the main axis, rosette diameter, height of the main axis, and length of the longest secondary inflorescence shoot. After scoring T2 plants, we harvested seed and grew a sample on kanamycin plates and used the ratio of Kan^r:Kan^s as a proxy for genotype of the scored T2 plant (all resistant, homozygous for the transgene; all sensitive, wild-type; quarter sensitive, hemizygous).

Three single locus transgenic lines and three EGFP fusion lines, all in a *tfl1* mutant background, were selected and selfed to yield homozygous lines for further phenotypic

characterization in the T4 generation. For phenotype scoring experiments, seedlings were germinated on 0.5× MS medium after 2 d of cold treatment. Plants were transferred to soil and grown at 23°C and *c.* 120 μmol m^{-2} s^{-1} under 16:8 h day:night photoperiod. Statistical analyses were conducted in Excel (Microsoft Corp., Redmond, WA, USA) and SigmaStat (Systat Software Inc., San Jose, CA, USA). A sample of 25 homozygous, *EGFP-LcrTFL1* plants in the T4 generation were examined using a confocal laser scanning microscope (Zeiss LSM 510 Meta) at a wavelength of 488 nm.

Quantitative reverse transcription polymerase chain reaction (RT-PCR)

Total RNA was extracted with PureYield™ RNA Midiprep System (Promega, Madison, WI, USA). RNase-free DNase (Fermenta, Glen Burnie, MD, USA) was used to eliminate genomic DNA contamination. First-strand cDNA synthesis was performed using ImProm-II™ Reverse Transcription System (Promega) with the oligo$(dT)_{15}$ primer. Real-time PCR was performed with the Brilliant SYBR Green QPCR Master Mix (Stratagene, Santa Clara, CA, USA) in a Stratagene MX3000P qPCR system. All PCR reactions were performed with the default program (94°C for 3 min, followed by 40 cycles of 94°C for 30 s, 55°C for 30 s, and 72°C for 1 min). The PCR reactions were followed by a dissociation curve analysis to verify there was no primer self-amplification. Primer sequences (all 5′ to 3′) were as follows: *LcrTFL1*, ATATGAGAAGTAGAGTGG GAGATC and GTGTTCTTTTAGAAAGGGGTCAC TA; *TFL1*, ATAGACCCAGATGTTCCA and ATGTA TCCCTATGCTTGG. Relative concentrations were normalized to QPCR reactions using actin control primers (Act1 5′-GTATTGTGTTGGACTCTGGTGATGGTGT-3′ and Act2 5′-GATGGATCCTCCAATCCGACACTGTA-3′).

Scanning electron microscopy

Living specimens were fixed in FAA (5% formalin, 5% acetic acid, and 47.5% ethanol in distilled water) and subsequently stored in 70% ethanol. Tissue samples were then dehydrated in an ethanol series, critical-point dried, sputter-coated with gold, and studied at 20 kV in an Environmental Scanning Electron Microscope (FEI Quanta 450, Hillsboro, OR, USA).

Results

Isolation of *LcrTFL1*

We searched the *L. crassa* genome for *TFL1* (At5G03840) homologs using PCR with degenerate primers. A 727 bp fragment with high similarity to *A. thaliana TFL1* was amplified and designated as *LcrTFL1* (*L. crassa* Terminal Flower 1). We used genome walking (Clontech) to isolate the full-length genomic sequence of the *LcrTFL1* locus (Genbank accession GU136396). The *LcrTFL1* locus has a similar structure to the *TFL1* locus (Fig. 2a). In the 5′ direction the closest gene to *LcrTFL1* is homologous to At5G03850, which is also the gene that is directly upstream of *TFL1*. In the 3′ direction, the closest gene model to *TFL1* is At5G03837, encoding a short hypothetical protein of 51 amino acids. Sequences 3′ of *LcrTFL1* also showed similarities to At5G03837. The inferred amino acid sequence of the *L. crassa* At5G03837 homolog is highly divergent from At5G03837, except for one 20 amino acid domain that shows > 75 amino acid identity. However, even in this domain the dN:dS ratio is *c.* 1.0, pointing to a lack of purifying selection. Combined with the absence of evidence of any transcript, we conclude that neither At5G03837 nor the corresponding region in *L. crassa* encodes functional genes. The next gene 3′ of *TFL1* is At5G03830, which is located just over 5 kb from the *TFL1* stop codon. We sequenced a little > 2.7 kb 3′ of *TFL1* but did not find any other open reading frames (ORFs).

Based on cDNA sequencing, it was determined that the intron–exon structure of *LcrTFL1* is identical to *TFL1*, although *LcrTFL1* introns are consistently shorter because of a number of small deletions (Fig. 2a). The cDNAs encode proteins of the same size (177 residues) that can be aligned without indels and with only 15 amino acid differences (Fig. 2b). The dN:dS ratio for the comparison of *LcrTFL1* and *TFL1* was 0.137. This value is much less than 1.0, showing that purifying selection has been acting on *TFL1* and that positive selection has been either absent or restricted to a small subset of sites. For comparison, the dN:dS ratio for *LcrLFY* vs *LFY* was 0.091, implying that *LFY* homologs have been subject to stronger purifying selection than *TFL1* homologs (or possibly that directional selection has acted on a greater subset of sites within TFL1 proteins).

To further confirm the orthology of *LcrTFL1* and *TFL1*, we generated an exon alignment for these two genes and other members of the *TFL1* gene family from a few other rosids. This alignment included additional homologs from *A. thaliana* (*FT*, *TSF*, *ATC*, *MFT* and *BFT*). Phylogenetic analysis of aligned DNA (Fig. S1) or amino acid sequences (Fig. S2) yielded a well-supported phylogenetic tree consistent with *LcrTFL1* being orthologous to *TFL1* (Fig. 2c).

In order to explore the potential for regulatory divergence between *TFL1* and *LcrTFL1*, we compared their flanking noncoding sequences. The 5′-intergenic region of *LcrTFL1* is only 966 bp, whereas that of *TFL1* is 2745 bp. As a result, many potential 5′ *cis*-regulatory elements are absent from *LcrTFL1*. Interestingly, a potential LFY binding site located 379 bp upstream of the *TFL1* start codon is missing in *LcrTFL1*. The 3′-intergenic regions of *LcrTFL1* and *TFL1* are highly divergent in sequence, making alignment impossible. We looked specifically for the two CArG boxes that have been implicated (in *A. thaliana*) as repressor sites that are bound by AP1 (Kaufmann *et al.*, 2010). The more distal repressor site, situated 1756 bp downstream of the stop codon in *A. thaliana*, was identified in *LcrTFL1* based on it having an identical sequence and sitting in the middle of a *c.* 120 bp region of high similarity between *LcrTFL1* and *TFL1* (Fig. S3). In *LcrTFL1* this distal repressor is situated 1032 bp downstream of the stop codon, showing that there has been a net deletion of 724 bp in the 3′-region of *LcrTFL1* relative to *TFL1*. This deletion may explain why the proximal *AP1* repressor site, situated 1011 bp downstream of the stop codon in *TFL1*, is not present in *LcrTFL1*.

LcrTFL1 replaces the function of Arabidopsis *TFL1* but causes novel phenotypes

The *LcrTFL1* genomic locus, including the entire 5′-intergenic region and 2704 bp of 3′ noncoding DNA, was introduced into *A. thaliana tfl1-2* mutant plants. We also generated constructs in which an *EGFP* domain was translationally fused to the 5′-end of the *LcrTFL1* coding region. All 28 *LcrTFL1* primary transformant (T1) plants carrying the genomic fragment showed full rescue of the mutant phenotype, with no terminal flowers observed. The 12 *EGFP-LcrTFL1* lines examined showed either complete rescue (no terminal flowers) or partial rescue (much delayed production of terminal flowers). The observation that both the genomic and fusion constructs prevent or greatly delay terminal flower formation shows that the LcrTFL1 protein is functional in *A. thaliana*, as might be expected given the two proteins' high amino acid similarity.

Compared with wild-type *A. thaliana*, *LcrTFL1* and *EGFP-LcrTFL1* lines also displayed some new traits. These included an increased number of secondary inflorescences, conversion of flowers into paraclades, short internodes in the primary inflorescence, shorter paraclades, and increased rosette leaf number (Fig. 3). These phenotypes were also observed in *35S:TFL1* transgenic plants, suggesting that they most likely reflect ectopic or expanded expression.

Although *LcrTFL1* transformant plants resembled *35S:TFL1* lines in many regards, some phenotypes were observed consistently in *LcrTFL1* lines but not in either *35S:TFL1* or wild-type *A. thaliana*: extra petals were formed in many flowers, specifically the earliest (lowermost) flowers produced on primary and secondary inflorescence axes (Fig. 3a–f); some flowers had elongated pedicels (Fig. 3b, c,g); some structures were formed that have features intermediate between flowers and paraclades (Fig. 3g); some cauline leaves lacked axillary paraclades (Fig. 3h); secondary inflorescence branches showed delayed elongation resulting in the transient formation of aerial rosettes (Fig. 3i). While the formation of aerial rosettes is not uncommon in *A. thaliana*, and seems to result from delayed elongation of paraclade shoots (Grbić & Bleecker, 2000), the other novel phenotypes suggest that the effects of *LcrTFL1* might not result just from elevated expression levels, but may also reflect modifications to the expression pattern and/or changes in protein function.

To see if *LcrTFL1* has a *trans*-dominant effect, we introduced the genomic construct into a wild-type *A. thaliana* background. To facilitate comparison with *35S:TFL1*, which is in the Columbia ecotype (Ratcliffe *et al.*, 1999), we used wild-type *A. thaliana* Col-0 as the recipient genome. The > 50 independent *LcrTFL1*/*Col-0* transgenic lines were examined and all showed a phenotype that closely resembled *LcrTFL1*/*tfl1-2* plants in the T1 generation. To quantify the phenotypic effects, we grew 30–50 seedlings from each of five T2 families without selection. A two-way ANOVA was used to assess whether the inferred genotype classes (wild-type, hemizygous, and homozygous for the transgene) differ significantly. A significant genotype effect was detected for all phenotypes, showing that the transgene does have a *trans*-dominant effect (Table S1). Post-hoc tests using Fisher's least significant difference showed that there are significant differences between wild-type plants and plants with at least one transgene, but they did not detect a significant difference between homozygous and hemizygous T2 plants for any phenotype. This result suggests that once one copy of *LcrTFL1* is present in the genome, the addition of a second copy has little additional impact on the phenotype. While quantitative variation was detected among T2 families, these differences were much smaller than the differences between transgenic plants and wild-type controls. This suggests that the transgenic phenotypes are relatively robust to between-line variation in expression level.

Plants from three homozygous *LcrTFL1* transgenic single-locus lines in a L*er tfl1-2* mutant background, one *LcrTFL1* transgenic single-locus line in a Col background, and three *EGFP-LcrTFL1* transgenic lines in a L*er tfl1-2* mutant background were grown in controlled conditions alongside *35S:TFL1*, *EGFP-TFL1*, *tfl1-2* and wild-type Col and L*er* lines. Table 1 summarizes some of the quantitative measurements that were made on these lines. *LcrTFL1* plants resembled *35S:TFL1* lines for many phenotypes, including an increased number of secondary inflorescence shoots, an increased number of cauline leaves, and late flowering. For these phenotypes *35S:TFL1* plants showed the strongest deviation from wild-type plants, followed by *LcrTFL1* lines, with *EGFP-TFL1* lines being closer to, but still significantly different from, wild-type lines.

Despite the overall similarities between *LcrTFL1* and *35S-TFL1* plants, there were some striking differences too. *LcrTFL1* consistently caused the production of additional petals in the lower flowers of the main axis, and similarly these early flowers had significantly longer pedicels than wild-type plants. For both phenotypes, an ANOVA detected a systematic tendency for more basal flowers to have more petals and longer pedicels than more apical ones. By contrast, *35S:TFL1* plants produced a normal number of petals and had significantly shorter pedicels than wild-type plants. Additionally, the lowest three internodes on the elongated portion of the inflorescence were found to be significantly shorter than the wild-type in *LcrTFL1* lines, but unchanged in *35S:TFL1* plants.

A more complex pattern was seen with regard to plant height: *LcrTFL1* plants were, like *35S:TFL1* plants, significantly taller than wild-type plants in a *tfl1* mutant L*er* background, but they were significantly shorter than wild-type plants when in a wild-type Col background. This difference correlates with the fact that, in a wild-type Col background, the *LcrTFL1* gene seems to reduce the number of cauline leaves, which is a proxy for the number of elongated internodes in the inflorescence.

LcrTFL1 shows expanded expression in *A. thaliana* transgenic lines

The broad similarities between *LcrTFL1* and *35S:TFL1 A. thaliana* plants led us to hypothesize that the *LcrTFL1* gene would show an elevated expression level and/or an expanded expression domain relative to *TFL1*, which is restricted to the vicinity of the inflorescence meristem at both the mRNA and protein levels (Bradley *et al.*, 1997; Conti & Bradley, 2007). Quantitative real-time RT-PCR (qPCR) showed that the quantity of transcript in the inflorescence of *LcrTFL1* lines normalized to an actin control (1.4 ± 0.14) was significantly higher than the equivalent tissue in wild-type *A. thaliana* (1.0 ± 0.07).

To assess the spatial pattern of expression of *LcrTFL1* in an *A. thaliana* background, we looked at the distribution of GFP fluorescence in 12 independent *EGFP-LcrTFL1* lines that showed complete or almost complete rescue of the *tfl1-2* mutation. Confocal microscopic analysis detected GFP fluorescence not only in inflorescence meristems but also in the outer layers of the inflorescence axis, pedicels, and flowers (Fig. 4). This contrasts with fluorescence observed in *Arabidopsis* plants transformed with an *EGFP-TFL1* construct (kindly provided by K. Goto), which show expression only in the inflorescence meristem (Fig. 4). Our construct, like the *EGFP-TFL1* construct, includes the full 5′-intergenic spacer and introns. However, because the *EGFP-TFL1* construct contains more sequences 3′ of the *TFL1* gene (5.3 kb) than did our *EGFP-LcrTFL1* construct (2.7 kb), we cannot rule out the possibility that we are missing a repressor element in this region of the *L. crassa* genome.

Scanning electron microscope observations show that *LcrTFL1* lines manifest a disrupted vegetative to reproductive transition

Scanning electron microscope (SEM) images of inflorescence meristems of *LcrTFL1* lines showed that the establishment of floral identity was delayed (Fig. 5). In a plant that had not yet bolted, the shoot apical meristem was found to resemble an inflorescence meristem surrounded by numerous lateral primordia (Fig. 5a). In a pattern reminiscent of broccoli, the lateral primordia seem to have adopted neither a clearly floral nor an inflorescence identity (Carr & Irish, 1997). Later, when bolting is under way, many of the lateral primordia have clearly adopted a floral identity, as indicated by calyx development (Fig. 5b–c). However, many flowers at this stage were observed to have additional sepal lobes. The extra sepals seen in young floral primordia contrasts with mature *LcrTFL1* flowers (Fig. 3a–b), which often have extra petals (Table 1) but were not observed to have extra sepals. While 35S:TFL1 inflorescence meristems are surrounded by more floral meristems at the time of bolting than are wild-type plants, these floral meristems proceed normally through the stages of flower development (Fig. 5d). These striking differences in early development between *LcrTFL1* and *35S:TFL1* lines imply that the architectural and floral anomalies of *LcrTFL1* lines cannot simply be explained by general ectopic expression of a TFL1 homolog but likely reflect more nuanced changes in expression and/or differences in protein function.

LcrTFL1/LcrLFY double transgenic lines resemble *LcrTFL1* lines, but show greater elongation of rosette-derived inflorescences

To explore the *in vivo* interaction between *LcrTFL1* and *LcrLFY*, *LcrTFL1/LcrLFY* double transgenic lines were made in both the *tfl1-2* and *lfy Arabidopsis* mutant backgrounds. There were made by transforming single-locus, homozgous *LcrTFL1 tfl1-2* lines with *LcrLFY* and

single-locus homozygous *LcrLFY lfy-6* lines with *LcrTFL1*. In the *lfy-6* mutant background, 19 of the 39 doubly transgenic T1 plants strong resembled *lfy* mutations (Fig. 6a,c), producing only flower-inflorescence intermediates (sometimes resembling broccoli), and lacking petals or stamens. Conversely, 22 of the 44 T1 lines in a *tfl1* mutant background made terminal flowers and/or bracteate flowers, resembling *tfl1* mutants (Fig. 6g). One hypothesis is that the balance of these two mutually antagonistic genes is finely balanced such that whichever gene starts at a lower background level of expression often becomes fully repressed, yielding plants that resemble the mutant.

The remainder of the double transgenic lines in both backgrounds resembled *LcrTFL1* lines, having delayed flowering and increased numbers of paraclades. Those lines that produced more or less normal flowers also produced flowers with extra petals (Fig. 6b,e,g) and often had elongated pedicels (Fig. 6f), like *LcrTFL1* single transgenic lines. While the double transgenic lines were qualitatively similar to *LcrTFL1* single transgenic lines, they showed an enhanced tendency to suppress axillary shoots associated with cauline leaves on elongated portions of the primary inflorescence (Fig. 6d,h). This was especially true in a *lfy* mutant background, where axillary shoots were often completely suppressed (Fig. 6d). At the same time, rosette-derived shoots tended to show extensive elongation (again, especially in a *lfy* background).

Among the many double transgenic lines, we selected two representative lines from each background for quantitative analysis in the T3 generation, avoiding lines that resembled either *lfy* or *tfl1*mutants. The lines chosen were inferred to be homozygous at a single locus for both transgenes. The double lines were scored for the same phenotypic traits as the single transgenic lines (Table 2). For most phenotypes, the double transgenic lines were intermediate between *LcrLFY* single and *LcrTFL1* single transgenic lines, although generally closer to *LcrTFL1*. This suggests that the ectopic activity of *LcrTFL1* is sufficient to overcome the enhanced activity and expression reported for *LcrLFY* (Yoon & Baum, 2004;Sliwinski *et al.*, 2006). However, the number of petals observed in the double lines was closer to *LcrLFY* single lines than to *LcrTFL1* single lines.

For petal number, pedicel length, internode length, number of secondary inflorescences, and number of cauline leaves, the effects of *LcrTFL1* were stronger in a *lfy* mutant background than in a *tfl1* background. This was particularly marked for internode length, which was only *c.* 20% of wild-type in a *lfy* background and 48% of wild-type in a *tfl1* background. These results suggest that the endogenous *TFL1* gene makes a much larger contribution to these phenotypes than does the endogenous *LFY* gene. Double transgenic lines had shorter inflorescences than the wild-type when in a *lfy* background, but were similar or slightly taller than the wild-type when in a *tfl1* background. This correlates with the data from single transgenic lines, where the presence of a functional endogenous copy of *TFL1* (i.e. in a wild-type background) in addition to the *LcrTFL1* transgene yielded shorter plants.

Discussion

We isolated *LcrTFL1* from the rosette-flowering crucifer, *L. crassa*, and showed that it is orthologous to the *A. thaliana* gene *TFL1*, as evidenced by genomic colinearity, high similarity in protein sequence, and the genes' sister-group relationship on the inferred phylogenetic tree. Introducing the *LcrTFL1* genomic region into a *tfl1* mutant, *A. thaliana* successfully rescued the terminal flower phenotype of *tfl1* mutants. Taken together, these data suggest that the LcrTFL1 and TFL1 proteins share a conserved biochemical function.

Introduction of the *LcrTFL1* genomic locus into *A. thaliana* mutants resulted in plants that resembled *35S:TFL1* transformants, consistent with the broad expression seen in *EGFP-*

TFL1 reporter lines. There are two possible interpretations of this expanded expression. The first possibility is that the expanded expression is a consequence of the *LcrTFL1* genomic fragment lacking an important repressor *cis*-regulatory element that is conserved between *L. crassa* and *A. thaliana*. In the 5′ direction, our *LcrTFL1* construct is like the *EGFP-TFL1* construct in that it includes the full 5′-intergenic spacer. This argues against there being a functionally and spatially conserved 5′ repressor element that could explain the additional expression of *LcrTFL1*. However, in the 3′ direction, the *EGFP-TFL1* construct contains a larger portion of noncoding DNA than does the *LcrTFL1* construct, so it is a formal possibility that the latter construct omits an important 3′ conserved repressor element. This could be tested with a chimeric construct that includes the full *LcrTFL1* construct plus the additional portion of 3′ noncoding DNA that is present in the *TFL1* construct but absent from the *LcrTFL1* construct.

The second possible explanation for the resemblance between the *LcrTFL1* and *35S:TFL1* plants is that there has been evolutionary divergence in the regulation of the expression of *TFL1* genes; for example, a repressor element may have been lost or an enhancer element gained on the *L. crassa* lineage some time since its last common ancestor with *A. thaliana*. One candidate element is the proximal *AP1* CArG repressor element, which is present in the 3′ noncoding region of *TFL1* but is absent in *LcrTFL1*. Kaufmann *et al.* (2010) showed that the proximal *AP1* repressor element, along with a more distal *AP1* repressor element that is conserved between the two species, has functional significance in *A. thaliana*. A second candidate is a predicted LFY-binding site, which is found at −379 bp in the 5′ noncoding DNA of *TFL1* but not in *LcrTFL1*. Future studies should examine whether the addition of the proximal *AP1* CArG site and/or the 5′ potential LFY-binding site to LcrTFL1 is sufficient to cause expression that more closely resembles *TFL1*. This will be interesting because such a finding would render it plausible that the up-regulation of *LcrTFL1* resulted from coevolution with interacting meristem identity genes (homologs of *LFY* and *AP1*), perhaps coincident with the evolution of rosette flowering.

While *LcrTFL1* lines resembled *35S:TFL1* in many regards (e.g. late flowering, homeotic conversion of paraclades into flowers), there were also some striking differences. Two of these novel traits, the accumulation of arrested lateral primordia of intermediate flower/paraclade identity (Fig. 5) and the production of flowers with extra petals (Fig. 3), do not resemble the donor species, *L. crassa*. The temporary arrest of lateral primordia is best interpreted as resulting from defects in the establishment of floral identity. Of several possible explanations, one worth mentioning is that the LcrTFL1 protein is a better repressor of flower meristem identity genes than is TFL1. This would mirror the finding that LcrLFY is better than LFY at activating early expression of *TFL1* (Sliwinski *et al.*, 2006). While this hypothesis remains speculative, it would be worth using expression analysis to investigate whether LcrTFL1 is more effective than TFL1 at repressing floral meristem identity genes such as *LFY* and *AP1*. Ideally, this experiment should be done with plants transformed with a construct that contains the *LcrTFL1* coding region surrounded by *A. thaliana cis*-regulatory sequences.

The production of extra petals in *LcrTFL1* lines resembles neither the wild-type species nor *35S:TFL1* plants, all of which produce classic, four-merous, crucifer flowers. The extra petal phenotype was also seen in *LcrLFY* lines (Yoon & Baum, 2004). *LcrTFL1*/*LcrLFY* doubly transgenic lines did not show synergy, petal number being similar to *LcrLFY* single transgenic lines. What should we make of a phenotype that is induced by the introduction of either of two genes from the same donor species, given that those two genes are largely antagonistic in function? One possibility is that *TFL1* and *LFY* genes work cooperatively via an additional, heretofore cryptic, pathway to regulate perianth development as a function of flower size. If this is true, introduction of either gene from the large-flowered *L. crassa*

could cause proliferation of the perianth. This explanation does not seem compelling, however, given the lack of reports of *TFL1* expression in the perianth. Another explanation worth considering is that the extra petals, which form in the lowermost flowers in inflorescence branches, are an indirect manifestation of defects in floral meristem identity establishment. Maybe these meristems transiently adopted a mixed flower-shoot identity resulting in some degree of proliferation of the outer parts of the primordia. Then, when floral identity was finally established, there may have been extra tissue that became assigned to new sepal lobe primordia (which later fuse to re-establish four organs) and new petal primordia. The latter hypothesis could be tested in part by conducting SEM investigations of *LcrLFY* lines to see if they too accumulate primordia of unclear identity during bolting. Additionally, it might be informative to drive expression of *LcrLFY* and *LcrTFL1* by perianth-specific promoters.

In contrast to disrupted vegetative-reproductive transition and extra petals, two other novel traits observed in *LcrTFL1* plants resemble the donor species: internode compression and pedicel elongation. Species in the *Leavenworthia* clade have compressed interfloral internodes on the main axis and elongated pedicels. We have previously hypothesized (Sliwinski *et al.*, 2007; Bosch *et al.*, 2008) that elevated expression of *LFY* genes contributed to internode compression along the main axis in rosette flowering species. The data presented here suggest that the *Leavenworthia* homologs of *TFL1* may also play a role in internode compression along the main axis. *LcrTFL1* plants had interfloral internodes that were significantly shorter than in wild-type plants. This effect is *trans*-dominant, being seen even in a wild-type background: *LcrTFL1* Col plants have internodes that are about half as long as wild-type Col plants. Double transgenic lines also have shorter internodes than wild-type lines, especially in a *lfy* mutant background where internodes are *c.* 20% of wild-type. Because the internode compression effect is not observed in *35S:TFL1* lines, it cannot be attributed simply to ectopic TFL1 activity. The use of chimeric constructs that combine the coding region of *TFL1* with the regulatory regions of *LcrTFL1* (or vice versa) would help determine whether the internode compression phenotype is caused by amino acid or regulatory differences within the *LcrTFL1* locus.

While we had no *a priori* reason to expect an effect of *LcrTFL1* on pedicel elongation, we noticed that *LcrTFL1* lines produced some flowers with unusually long pedicels. Quantitative analyses showed that the lower five flowers have significantly longer pedicels in singly or doubly transgenic *LcrTFL1* lines than in wild-type lines, whereas *35S:TFL1* lines resemble wild-type lines. This effect was, again, *trans*-dominant, being seen in the presence of a functional endogenous *TFL1* gene. This result suggests that the modulation of meristem identity genes not only can affect architecture in the narrow sense, but also can influence plant structure by affecting the relative elongation of different stem regions (pedicels vs internodes).

Our data are compatible with the claim that changes in *LcrTFL1* and *LcrLFY* contributed to the evolution of several aspects of the derived architecture of *Leavenworthia*, most notably internode compression and pedicel elongation. However, even if this is so (which remains to be shown), our data also clearly show that *LcrTFL1* and *LcrLFY* could not have been the sole target of developmental evolution. If they were, the double transgenic lines would closely approach the rosette-flowering form of *L. crassa*, which they certainly do not. The insufficiency of *LcrTFL1* and *LcrLFY* to recapitulate rosette flowering in *Leavenworthia* shows that even if these two genes were important in the evolution of rosette flowering, other genes played additional essential roles. Further work on interacting genes, most obviously *APETALA1* (Kaufmann *et al.*, 2010), is needed to explain how an evolutionary change from inflorescence to rosette flowering was achieved without disrupting critical processes such as the formation of normal, fully functional flowers.

Supplementary Material

Refer to Web version on PubMed Central for supplementary material.

Acknowledgments

The authors gratefully acknowledge the following for technical support and advice: Justin Bosch, Ivalú Cacho, Donna Fernandez, Ruth Litovsky, Abigail Mazie, Kevin Miller, Rebecka Pralle, R. Pulikesi, Sara Swanson and Amanda Teschke. Biological materials were kindly provided by Enrico Coen, Koji Goto, Angela Hay and Miltos Tsiantis. Assistance in the preparation of graphics was provided by Claudia Lipke and Kandis Elliot. This work was funded by the National Science Foundation (IOB-0641428).

References

Ahn JH, Miller D, Winter VJ, Banfield MJ, Lee JH, Yoo SY, Henz SR, Brady RL, Weigel D. A divergent external loop confers antagonistic activity on floral regulators *ft* and *tfl1*. EMBO Journal 2006;25:605–614. [PubMed: 16424903]

Baum DA, Yoon HS, Oldham RL. Molecular evolution of the transcription factor *LEAFY* in *Brassicaceae*. Molecular Phylogenetics and Evolution 2005;37:1–14. [PubMed: 16112883]

Benlloch R, Berbel A, Serrano-Mislata A, Madueño F. Floral initiation and inflorescence architecture: a comparative view. Annals of Botany 2007;100:659–676. [PubMed: 17679690]

Bosch JA, Heo K, Sliwinski MK, Baum DA. An exploration of LEAFY expression in independent evolutionary origins of rosette flowering in *Brassicaceae*. American Journal of Botany 2008;95:286–293.

Bradley D, Carpenter R, Copsey L, Vincent C, Rothstein S, Coen E. Control of inflorescence architecture in *Antirrhinum*. Nature 1996;379:791–797. [PubMed: 8587601]

Bradley D, Ratcliffe O, Vincent C, Carpenter R, Coen E. Inflorescence commitment and architecture in *Arabidopsis*. Science 1997;275:80–83. [PubMed: 8974397]

Carr SM, Irish VF. Floral homeotic gene expression defines developmental arrest stages in *Brassica oleracea* L. vars. *botrytis* and *italica*. Planta 1997;201:179–188. [PubMed: 9084216]

Clough SJ, Bent AF. Floral dip: a simplified method for *Agrobacterium*-mediated transformation of *Arabidopsis thaliana*. Plant Journal 1998;16:735–743. [PubMed: 10069079]

Coen ES, Nugent JM. Evolution of flowers and inflorescences. Development 1994;(Suppl):107–116.

Conti L, Bradley D. TERMINAL FLOWER1 is a mobile signal controlling *Arabidopsis* architecture. Plant Cell 2007;19:767–778. [PubMed: 17369370]

Grbić V, Bleecker AB. Axillary meristem development in *Arabidopsis thaliana*. Plant Journal 2000;21:215–223. [PubMed: 10743661]

Huelsenbeck JP, Ronquist F. MrBayes: Bayesian inference of phylogenetic trees. Bioinformatics 2001;17:754–755. [PubMed: 11524383]

Kaufmann K, Wellmer F, Muiño JM, Ferrier T, Wuest SE, Kumar V, Serrano-Mislata A, Madueño F, Krajewski P, Meyerowitz EM, et al. Orchestration of floral initiation by APETALA1. Science 2010;328:85–89. [PubMed: 20360106]

Kumar S, Nei M, Dudley J, Tamura K. Mega: a biologist-centric software for evolutionary analysis of DNA and protein sequences. Brief Bioinformation 2008;9:299–306.

Kumar S, Tamura K, Nei M. Mega: molecular evolutionary genetics analysis software for microcomputers. Computer Applications in the Biosciences 1994;10:189–191. [PubMed: 8019868]

Maddison, DR.; Maddison, WP. MacClade 4: analysis of phylogeny and character evolution. Sunderland, MA, USA: Sinauer; 2002.

Miller, MA.; Holder, MT.; Vos, R.; Midford, PE.; Liebowitz, T.; Chan, L.; Hoover, P.; Warnow, T. The CIPRES portal. CIPRES. 2009 [accessed on 4 August 2009]. [WWW document].URL http://www.phylo.org/sub_sections/portal. Archived by WebCite(r) at http://www.webcitation.org/5imQlJeQa

Prusinkiewicz P, Erasmus Y, Lane B, Harder LD, Coen E. Evolution and development of inflorescence architectures. Science 2007;316:1452–1456. [PubMed: 17525303]

Ratcliffe OJ, Bradley DJ, Coen ES. Separation of shoot and floral identity in *Arabidopsis*. Development 1999;126:1109–1120. [PubMed: 10021331]

Ronquist F, Huelsenbeck JP. MrBayes 3: Bayesian phylogenetic inference under mixed models. Bioinformatics 2003;19:1572–1574. [PubMed: 12912839]

Shu G, Amaral W, Hileman LC, Baum DA. *LEAFY* and the evolution of rosette flowering in violet cress (*Jonopsidium acaule*, Brassicaceae). American Journal of Botany 2000;87:634–641. [PubMed: 10811787]

Sliwinski MK, Bosch JA, Yoon HS, Balthazar M, Baum DA. The role of two *LEAFY* paralogs from *Idahoa scapigera* (Brassicaceae) in the evolution of a derived plant architecture. Plant Journal 2007;51:211–219. [PubMed: 17559504]

Sliwinski MK, White MA, Maizel A, Weigel D, Baum DA. Evolutionary divergence of *LFY* function in the mustards *Arabidopsis thaliana* and *Leavenworthia crassa*. Plant Molecular Biology 2006;62:279–289. [PubMed: 16915521]

Smyth DR, Bowman JL, Meyerowitz EM. Early flower development in *Arabidopsis*. Plant Cell 1990;2:755–767. [PubMed: 2152125]

Thompson JD, Higgins DG, Gibson TJ. Clustal W – improving the sensitivity of progressive multiple sequence alignment through sequence weighting, position-specific gap penalties and weight matrix choice. Nucleic Acids Research 1994;22:4673–4680. [PubMed: 7984417]

Tucker S, Grimes J. The inflorescence: introduction. The Botanical Review 1999;65:303–316.

Yoon HS, Baum DA. Transgenic study of parallelism in plant morphological evolution. Proceedings of the National Academy of Sciences, USA 2004;101:6524–6529.

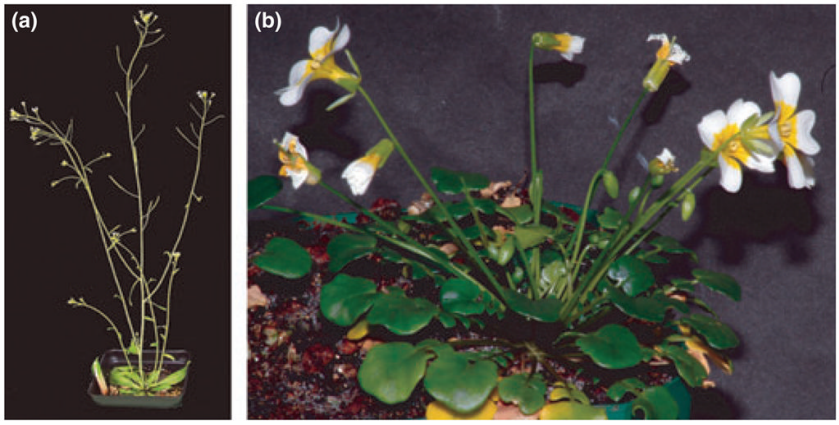

Fig. 1.
Comparison of the inflorescence-flowering species *Arabidopsis thaliana* (a) with the partially rosette-flowering species *Leavenworthia crassa* (b).

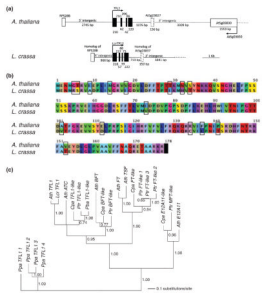

Fig. 2. Leavenworthia crassa TFL1

(*LcrTFL1*) is orthologous to the *Arabidopsis thaliana* gene *TFL1*. (a) Structure of the *LcrTFL1* and *TFL1* loci. (b) Alignment of the inferred protein sequences of LcrTFL1 and TFL1. The amino acid differences are boxed. (c) A phylogenetic tree estimate from the coding sequences (CDS) of various members of the TFL1 gene family. This tree is a majority-rule consensus tree based on the post-burn-in tree from two Bayesian Markov chain Monte Carlo runs of 2 000 000 generations each, applying the generalized time-reversible (GTR) + Γ model of molecular evolution. Values on branches are clade posterior probabilities. Branch lengths (substitutions/site) are the mean branch lengths across trees in the posterior that have the branch. Bayesian analysis of the amino acid sequence from the same genes (using the Whelan and Goldman (WAG) model of protein evolution) yielded a similar tree except that ATC was resolved as sister to Cpa TFL1-like with a 0.99 posterior probability.

Fig. 3.

Phenotypes of *Arabidopsis thaliana* plants transformed with *Leavenworthia crassa TFL1* (*LcrTFL1*). Close-up photographs show various recurrent features of *LcrTFL1* lines, including extra petals (a–g), production of elongated pedicels (b, c, g), production of occasional flower-shoot intermediates (c–d), and cauline leaves lacking associated paraclades (arrow in h). Comparison of *LcrTFL1* and control lines (i) shows that the *tfl1-2* mutation has been fully rescued and that *LcrTFL1* lines have many similarities to *35S:TFL1* lines.

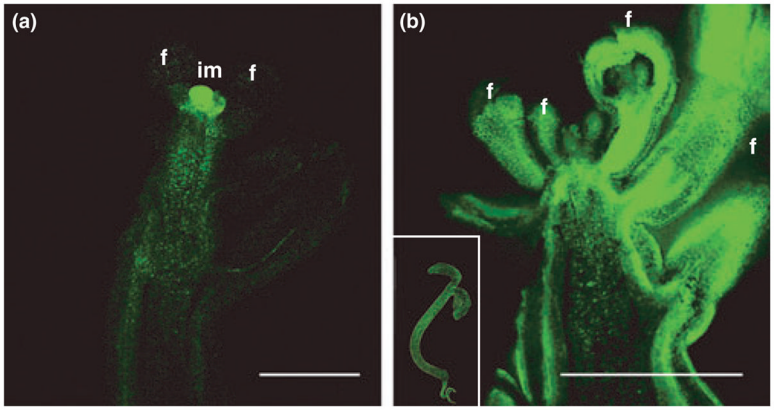

Fig. 4.

Localization of fluorescence in *EGFP-TFL1* and *EGFP-Leavenworthia crassa TFL1* (*EGFP-LcrTFL1*) lines. *TFL1* expression was restricted to the inflorescence meristem (a). By contrast, *LcrTFL1* was expressed in the inflorescence apex, floral organs, stem tissue (b) and throughout seedlings (b, inset). im, Inflorescence meristem; f, flower primordium. Bar, 500 μm.

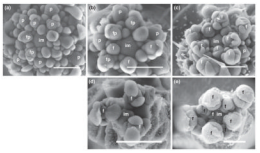

Fig. 5.

Scanning electron micrographs of primary inflorescence apices show disruptions of the floral transition in *Leavenworthia crassa TFL1* (*LcrTFL1*) lines compared with controls. In *LcrTFL1* plants that have not yet bolted (a), dissection reveals that the primary inflorescence meristem is surrounded by numerous primordia, most of which resemble floral primordia in stage 2 (stages defined by Smyth *et al.*, 1990). When the inflorescence shoots of *LcrTFL1* lines are *c.* 3 cmin height (b), many lateral primordia around the meristem still resemble stage 2–3 floral primordia, whereas others have an aspect intermediate between a paraclade and a stage 4 flower. When *LcrTFL1* lines reach 9 cmin height (c), most primordia resemble stage 4–6 floral primordia except that the sepal whorl is irregular and there are usually more than four sepal lobes. By contrast, when 3 cmbolts are observed in *35S:TFL1* (d) or wild-type lines (e), they are similar, each containing normal stage 5 and above floral primordia. im, Inflorescence meristem; f, flower primordium; p, paraclade; fp, shoot of uncertain, flower or paraclade identity. Bar, 200 μm.

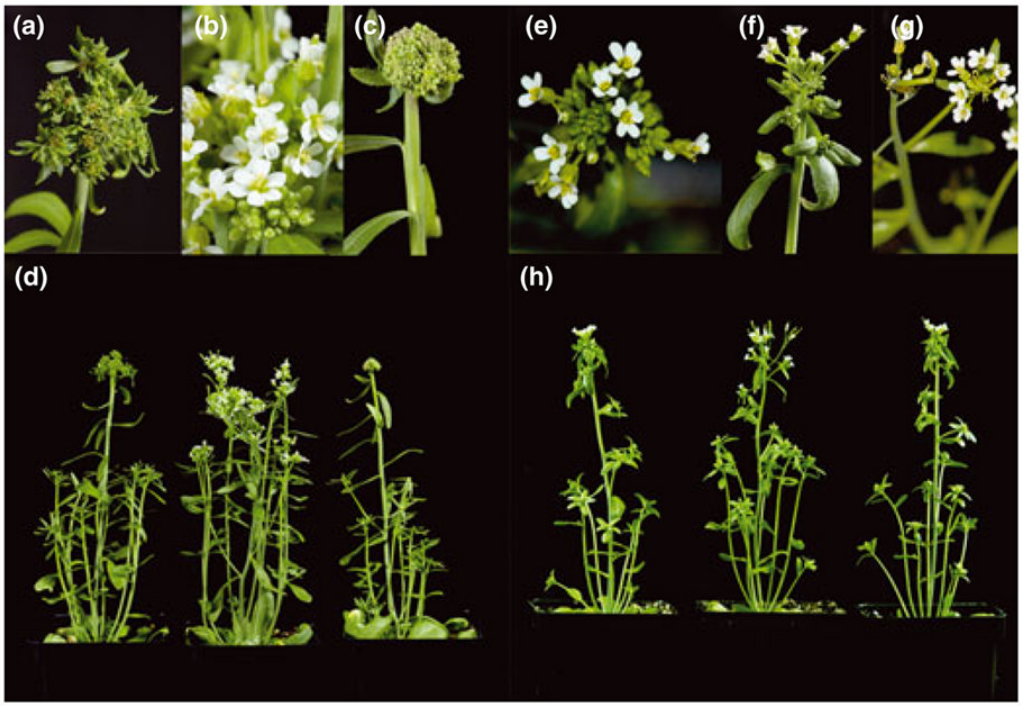

Fig. 6.

Phenotypes of *Leavenworthia crassa TFL1*/*L. crassa LFY* ortholog (*LcrTFL1*/*LcrLFY*) double transgenic lines in a *lfy* (a–d) or *tfl1* (e–h) mutant background. Phenotypes of *LcrTFL1*/*LcrLFY*/*lfy* transgenic lines are variable. Approximately half of the lines failed to form fertile flowers, instead forming compressed leafy axes (a) or broccoli-like inflorescences with apetalous flowers (c). In some cases, inflorescence stems lacked any paraclades (d). When flowers were formed, the earliest flowers tended to make extra petals (b). Phenotypes of *LcrTFL1*/*LcrLFY*/*tfl1* transgenic lines exhibited primarily *LcrTFL1*-like phenotypes, including extra petals (e), conversion of flowers into shoots (f), and long pedicels (e– f). Some lines, however, produced terminal flowers (g).

Table 1

Effect of *TFL1* and *LFY* transgenes on selected traits *Arabidopsis thaliana*

Ecotype	Genotype	Petals[a] (*n* = 9)	Pedicel[b] (cm) (*n* = 10)	Internode[c] (cm) (*n* = 5)	Inflorescence height (cm) (*n* = 16)
L*er*	Wild-type	4.04 ± 0.07	1.31 ± 0.04	1.40 ± 0.24	37.12 ± 0.35
	lfy-6	3.98 ± 0.05	1.01 ± 0.06**	0.97 ± 0.21	31.96 ± 0.53**
	tfl1-2	4.18 ± 0.28	0.84 ± 0.10**	1.13 ± 0.43	10.74 ± 0.62**
	LcrLFY L3-15.7	6.18 ± 0.57**	0.70 ± 0.04**	1.50 ± 0.42	25.26 ± 1.96**
	LcrTFL1 L1	4.98 ± 0.17**	1.47 ± 0.08**	0.50 ± 0.13**	45.78 ± 0.46**
	LcrTFL1 L2	5.02 ± 0.23**	1.55 ± 0.08**	0.42 ± 0.13**	46.59 ± 0.56**
	LcrTFL1 L16	4.84 ± 0.20**	1.54 ± 0.12**	0.67 ± 0.07**	40.61 ± 1.07*
	eGFP-LcrTFL1 L2.5	4.80 ± 0.17**	1.46 ± 0.06**	0.61 ± 0.14**	43.47 ± 1.21**
	eGFP-LcrTFL1 L41.2	4.96 ± 0.17**	1.46 ± 0.06**	0.47 ± 0.15**	44.16 ± 1.17**
	eGFP-LcrTFL1 L24.1	4.84 ± 0.14**	1.50 ± 0.06**	0.47 ± 0.15**	42.27 ± 1.31*
Col-0	Wild-type	3.98 ± 0.05	1.57 ± 0.06	2.11 ± 0.39	57.08 ± 0.48
	35S:TFL1	4.02 ± 0.05	1.38 ± 0.09**	2.11 ± 0.17	74.19 ± 0.78**
	GFP-TFL1	4.0 ± 0.07	1.55 ± 0.04	2.25 ± 0.37	48.86 ± 0.63**
	LcrTFL1	5.1 ± 0.21**	1.70 ± 0.09**	1.02 ± 0.14**	51.34 ± 1.03**

Ecotype	Genotype	Secondary inflorescences[d] (*n* = 16)	Cauline leaves[e] (*n* = 16)	Flowering time (d) (*n* = 16)	Flowering node[f] (*n* = 16)
L*er*	Wild-type	2.38 ± 0.13	2.31 ± 0.13	19.88 ± 0.22	12.50 ± 0.35
	lfy-6	2.88 ± 0.16	2.88 ± 0.16*	20.06 ± 0.21	11.13 ± 0.26
	tfl1-2	0.56 ± 0.18**	1.94 ± 0.19	13.13 ± 0.29**	8.38 ± 0.26**
	LcrLFY L3-15.7	1.81 ± 0.25	1.75 ± 0.27	21.00 ± 0.34	10.75 ± 0.36*
	LcrTFL1 L1	19.63 ± 0.43**	10.50 ± 0.21**	32.44 ± 0.50**	19.06 ± 0.57**
	LcrTFL1 L2	27.75 ± 1.06**	12.88 ± 0.41**	31.94 ± 0.50**	19.13 ± 0.36**
	LcrTFL1 L16	19.19 ± 1.74**	11.06 ± 0.54**	30.25 ± 0.60**	18.25 ± 0.76**
	eGFP-LcrTFL1 L2.5	10.69 ± 0.51**	6.50 ± 0.35**	29.63 ± 0.42**	15.88 ± 0.56**
	eGFP-LcrTFL1 L41.2	11.19 ± 0.46**	7.19 ± 0.26**	28.81 ± 0.39**	17.50 ± 0.32**

Ecotype	Genotype	Petals[a] (*n* = 9)	Pedicel[b] (cm) (*n* = 10)	Internode[c] (cm) (*n* = 5)	Inflorescence height (cm) (*n* = 16)
	eGFP-LcrTFL1 L24.1	11.19 ± 0.42**	6.38 ± 0.30**	28.38 ± 0.46**	16.63 ± 0.49**
Col-0	Wild-type	2.94 ± 0.14	2.94 ± 0.14	22.75 ± 0.22	15.88 ± 0.46
	35S:TFL1	52.75 ± 1.13**	12.25 ± 0.47**	46.69 ± 0.40**	36.81 ± 0.40**
	GFP-TFL1	2.44 ± 0.18	2.31 ± 0.12*	20.63 ± 0.24**	14.25 ± 0.30*
	LcrTFL1	44.50 ± 1.56**	11.79 ± 0.57**	32.36 ± 0.35**	19.81 ± 0.35

Each value represents the mean ± 1 SEM. Asterisks indicate a significant difference between the transgenic line and the corresponding wild-type as judged using either two-way ANOVA (petal number, pedicel length, internode length) or Student's *t*-test.

*Significantly different from the wild-type control ($P < 0.01$);

**significantly different from the wild-type control ($P < 0.001$).

[a]The numbers of petals in the first five flowers of the primary inflorescence were counted.

[b]The pedicel lengths of the first five flowers of the primary inflorescence were measured.

[c]The lengths of the first three floral internodes in the primary inflorescence were measured.

[d]Number of lateral shoots emerging from the main axis, whether from the rosette or inflorescence.

[e]Number of leaves on the elongated portion of the main axis.

[f]Nodes are defined as the number of leaves plus any lateral shoots that lack subtending leaves.

Table 2

Morphology of *Leavenworthia crassa LFY* ortholog/*L. crassa TFL1* (*LcrLFY LcrTFL1*) doubly transgenic plants in either the *tfl1-2* or *lfy-6* mutant background

Line	**Genetic background**	**Petals[a] (*n* = 9)**	**Pedicel[b] (cm) (*n* = 10)**	**Internode[c] (cm) (*n* = 5)**	**Inflorescence height (cm) (*n* = 16)**
L*er*	*LFY TFL1*	4.04 ± 0.07	1.31 ± 0.04	1.40 ± 0.24	37.12 ± 0.35
L3L3	*lfy TFL1*	5.98 ± 0.23**	1.56 ± 0.12**	0.27 ± 0.07**	nd
L3L4	*lfy TFL1*	5.89 ± 0.16**	1.26 ± 0.05	0.28 ± 0.04**	29.62 ± 1.87*
G16	*LFY tfl1*	5.73 ± 0.15**	1.68 ± 0.08**	0.63 ± 0.17**	38.38 ± 1.24
Y10	*LFY tfl1*	5.29 ± 0.27**	1.73 ± 0.07**	0.64 ± 0.18**	41.36 ± 0.78**
Line	Genetic background	Secondary inflorescences[d] (*n* = 16)	Cauline leaves[e] (*n* = 16)	Flowering time (d) (*n* = 16)	Flowering node[f] (*n* = 16)
L*er*	*LFY TFL1*	2.38 ± 0.13	2.31 ± 0.13	19.88 ± 0.22	12.50 ± 0.35
L3L3	*lfy TFL1*	nd	nd	nd	nd
L3L4	*lfy TFL1*	27.00 ± 1.87**	15.31 ± 2.30**	30.88 ± 0.34**	20.13 ± 0.76**
G16	*LFY tfl1*	9.94 ± 0.34**	5.94 ± 0.24**	29.56 ± 0.58**	18.39 ± 0.26**
Y10	*LFY tfl1*	12.00 ± 0.58**	7.83 ± 0.57**	30.06 ± 0.28**	18.22 ± 0.55**

Each value represents the mean ± 1 SEM. Asterisks indicate a significant difference between the transgenic line and the corresponding wild-type as judged using either two-way ANOVA (petal number, pedicel length, internode length) or Student's *t*-test.

*Significantly different from the wild-type control ($P < 0.01$);

**significantly different from the wild-type control ($P < 0.001$).

[a]The numbers of petals in the first five flowers of the primary inflorescence were counted.

[b]The pedicel lengths of the first five flowers of the primary inflorescence were measured.

[c]The lengths of the first three floral internodes in the primary inflorescence were measured.

[d]Number of lateral shoots emerging from the main axis, whether from the rosette or inflorescence.

[e]Number of leaves on the elongated portion of the main axis.

[f]Nodes are defined as the number of leaves plus any lateral shoots that lack subtending leaves. nd, not determined.